Effect of Annealing on the Deformation Mechanism of a Styrene/*n*-Butyl Acrylate Copolymer Latex Film Investigated by Synchrotron Small-Angle X-ray Scattering

Jianqi Zhang,[†] Shanshan Hu,[†] Jens Rieger,[‡] Stephan V. Roth,[§] Rainer Gehrke,[§] and Yongfeng Men*,[†]

State Key Laboratory of Polymer Physics and Chemistry, Changchun Institute of Applied Chemistry, Chinese Academy of Sciences, Graduate School of Chinese Academy of Sciences, Renmin Street 5625, 130022 Changchun, P. R. China; BASF SE, Polymer Physics, 67056 Ludwigshafen, Germany; and HASYLAB am DESY, Notkestrasse 85, 22607 Hamburg, Germany

Received February 27, 2008; Revised Manuscript Received April 9, 2008

ABSTRACT: The deformation mechanism of a styrene/*n*-butyl acrylate copolymer latex film subjected to uniaxial tensile stress was studied by small-angle X-ray scattering. The influence of annealing at 23, 60, 80, and 100 °C for 4 h on microscopic deformation processes was elucidated. It was demonstrated that the microscopic deformation mechanism of the latex films transformed gradually from nonaffine deformation behavior to affine deformation behavior with increasing annealing temperature. This behavior was attributed to the interdiffusion of polymeric chains between adjacent latex particles in the film, the extent of which increases with annealing temperature. The polycrystalline structure of the latex films was preserved even after annealing for 4 h at temperatures 80 K above the glass transition temperature; i.e., the structure is not completely homogenized by interdiffusion.

Introduction

Latices are dispersions of polymeric particles in a suspending medium, usually water. They are widely used in the form of films (after the water is evaporated) in many applications, such as paints, paper coatings, adhesives etc.[1] Often crystalline packing of the polymeric particles is observed when the latex dispersions are dried. The drying process may be divided roughly into three stages: increasing the particle concentration and ordering, particle deformation, and polymer chain diffusion across particle boundaries.[2,3] Latex particles assuming dodecahedral shape in the deformed state are usually packed in a face-centered cubic (fcc) structure.[4–8]

The diameter of the polymer particles in a latex dispersion lies in the range 10 nm to 100 μm with a typical size on the order of 100 nm,[9] resulting in a lattice spacing of the colloid crystals that is much larger than that of atomic or molecular crystals. The size of the building blocks of the colloid crystals and the contrast provided by the electron density difference between latex particles and nonpolymeric material like salt and surfactants, which is located in the interstices, make small-angle scattering techniques ideal for the structural investigation.[10–14] Studies have mainly focused on the structural evolution during the film formation process.[10–14] It has been found that the third step of film formation, namely the interdiffusion of the polymeric chains between adjacent particles, normally occurs during annealing at temperatures above the glass transition temperature. Small-angle neutron scattering (SANS) and fluorescence techniques have been two basic methods to investigate the diffusion of polymer molecules across the interface between adjacent particles in latex systems. In SANS experiments the interdiffusion behavior was studied through measurements on latex blends made from deuterated and protonated latex particles, while in fluorescence investigations polymer diffusion was studied by direct nonradiative energy transfer measurements using latex films comprised of two types of particles: one labeled with a donor dye and the other with an acceptor. As early as 1986, an increase in the radius of gyration of polymer chains during annealing, which provided evidence for interdiffusion between latex particles, was found by Hahn et al.[15] Since then, more advanced studies have been performed, including studies on the effect of temperature and molecular weight,[16,17] polymer composition,[18,19] the influence of coalescing aids,[20] and nonionic surfactants,[21,22] and on the influence of latex structure on the interdiffusion process.[23–25]

Although the final application of the polymeric latex films requires a thorough understanding of their structural behavior upon mechanical loading, up to now, studies on the deformation mechanism of polymer latex films are scarce. Lepizzera et al.[26,27] presented evidence for two types of deformation behavior, including matrix deformation and geometric rearrangement, through a research of morphology of deformed core/shell latex films by atomic force microscopy. Cabane et al.[28] studied the deformation of cellular polymeric films with SANS; they pointed out that the deformation was affine when the films were stretched in the dry state, while the macroscopic stretching caused microscopic shear deformation (i.e., the cells slipped past each other) in the wet state. We reported that stretching a soft latex film resulted not only in large deformation of the crystallographic unit cells but also in considerable nonaffine deformation at high draw ratios which was attributed to slippage between rows of particles and crystalline grain boundaries.[29] It has also been reported[30,31] that the pH value of the latex dispersions, volume fraction, and size of added silica particles affected the deformation mechanism in hybrid nanocomposite films.

In the present work, the effect of annealing on the deformation mechanism of the colloid crystal structure in a latex film was studied by means of synchrotron small-angle X-ray scattering (SAXS). The SAXS measurements indicated that the polycrystalline fcc structure was preserved after annealing at different temperatures above the glass transition temperature of the latex. Furthermore, it was found that the deformation mechanism of the latex films transformed from nonaffine deformation to affine deformation with increasing annealing temperature. This transformational behavior was attributed to the diffusion of polymeric

* Corresponding author. E-mail: men@ciac.jl.cn.
[†] Chinese Academy of Sciences.
[‡] BASF SE, Polymer Physics.
[§] HASYLAB am DESY.

10.1021/ma800435f CCC: $40.75 © 2008 American Chemical Society
Published on Web 05/16/2008

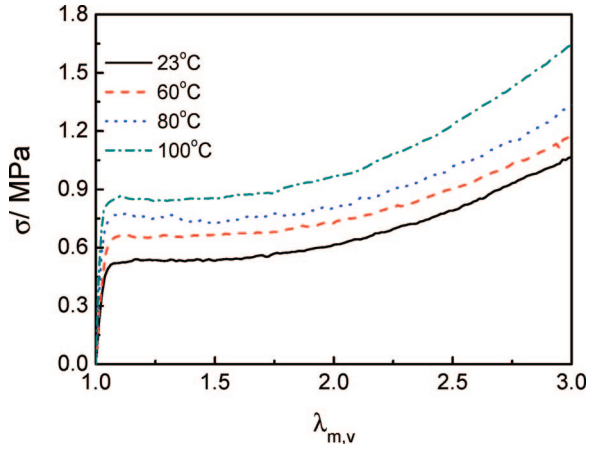

Figure 1. Stress−strain curves for latex films annealed at different temperatures.

chains between adjacent latex particles, resulting in an enhancement of the cohesive bonding between particles in the crystallites and at the grain boundaries.

Experimental Section

A styrene/*n*-butyl acrylate copolymer (PS-*co*-BA) latex dispersion with a solid content of ca. 40 wt % was used.[32] The glass-transition temperature of this PS-*co*-BA is 20 °C. The diameter of the latex particles is 118 nm as determined by SAXS. The latex films were obtained by evaporating the water from the latex dispersion at ambient condition (23 °C and 30% relative humidity) for 2 weeks, yielding a transparent film of about 1 mm thickness. The samples were cut into 15 mm length and 3 mm width. They were annealed at 23, 60, 80, and 100 °C for 4 h.

Synchrotron SAXS measurements were performed at the beamline BW4 at HASYLAB, DESY, Hamburg, Germany. The energy of the X-ray radiation was 8.979 keV, resulting in a wavelength of 0.138 08 nm. The size of the primary X-ray beam at the sample position was 0.4 × 0.4 mm^2. The sample was mounted onto a tensile tester at the beamline at a sample to detector distance of 5694 mm. At this distance, the effective scattering vector q ($q = 4\pi/\lambda \sin\theta$, where 2θ is the scattering angle and λ the wavelength) range is 0.03−0.62 nm^{-1}. The samples were stretched with a speed of 30 μm/s with a specially designed ministretcher. The samples were stretched at both ends, ensuring that the X-rays were scattered at a fixed position in the middle of the sample. The stretching force was recorded via a load cell of 10 N capacity attached to one of the clamps. Each SAXS pattern was collected within 60 s during a continuous stretching run. The SAXS data were calibrated for background scattering and normalized with respect to the primary beam intensity.

Results and Discussion

Figure 1 presents stress−strain curves for samples annealed at different temperatures. It can be seen that the curves have similar shapes that are typical for viscoelastic materials. Initially, the tensile stress increases rapidly at small deformations before reaching a strain softening point at a draw ratio of $\lambda_{m,v} =$ 1.05−1.08 ($\lambda_{m,v} = l/l_0$ where l_0 and l are the length of the latex film before and after stretching, respectively). After this yielding range, a gradual increase in stress is observed at larger draw ratios. Comparing the curves for samples annealed at different temperatures, one finds a shift of the stress−strain curves to larger stress values with increasing annealing temperature. This behavior is explained by assuming that the interdiffusion of polymer chains proceeded to different extents at different annealing temperatures, resulting in increased homogeneity and strength of the material with increasing interdiffusion (see below).

In order to elucidate the deformation mechanism before and after annealing, SAXS measurements were conducted. Selected SAXS patterns taken at different draw ratios for latex films annealed at different temperatures are given in Figure 2. They show typical powder diffraction features of the Debye−Scherrer ring type at $\lambda_{m,v} = 1$. The observed strong SAXS signal might appear at first sight quite unusual when considering prior models of latex film formation. It has been described that in the last stages of drying the system undergoes an inversion from an "oil-in-water" to a "water-in-oil" structure, where the terminology of emulsion science is used; "oil" denotes the hydrophobic polymer phase. In the "water-in-oil" structure the remaining water containing salts and surfactants forms droplet occlusions in the film. Because of the emulsion inversion, the liquid membranes between the particles disappear and the polymer material from adjacent particles comes into intimate contact, leading to the disappearance of Bragg reflections.[33,34] The strong SAXS signal observed in the current system has its origin from the specific composition of the latex particles that differs from the above systems. Distler and Kanig[35] showed that the distribution of monomers in similar latex systems is not homogeneous. More hydrophilic monomers tend to accumulate at the surface of the particles. When the latex particles contain a substantial amount of polar polymers bound to the surface, the inversion from "oil-in-water" to "water-in-oil" is prevented, and the particles in the film are separated by a membrane of polar material, leading to the type of Bragg reflections seen here by SAXS. The following observations are made in the present case; first, the q value of each ring increases with increasing annealing temperature, indicating a shrinkage of the crystalline lattice. This may be caused by coalescence of the particles accompanied by the expulsion of material that is not compatible with the latex polymers, such as surfactants which are initially covering the surface of the latex particles, into the interstices, upon annealing at elevated temperature.[36]

Second, it was found that the diffraction rings gradually became ellipses with increasing deformation—with the short axis in the stretching direction. The dimensions of the ellipses are proportional to the inverse dimensions of the unit cell of the structure.[28] In order to demonstrate the changes of q values along and perpendicular to the stretching direction quantitatively, 1D SAXS intensity distributions of the latex films obtained by integrating the intensity within a thin rectangular box along the respective directions are plotted in Figure 3, including data for samples before and after annealing. In the diagram only relative intensities are given, and spectra are vertically shifted for the sake of clarity. The Miller indices of the corresponding peaks are given in the plot. The shift of the corresponding q positions to larger values in undeformed samples upon annealing is clearly identifiable. Shifts of the q positions parallel and perpendicular to the stretching direction after deformation for both cases can be directly read out from the data.

In order to obtain the relation between the microscopic deformation, as indicated by the shift of the positions of the Bragg peaks, and the macroscopic deformation ratio, three diffraction peaks were followed during deformation along and perpendicular to the stretching direction. The corresponding draw and compression ratios of the crystalline lattices along and perpendicular to the stretching direction were derived from the 1D scattering intensity distributions as a function of the respective q. The results are shown in Figure 4.

It was found that the deformation was close to affine for all samples irrespective of the annealing temperature at small draw ratios ($\lambda_{m,v} < 1.5$); i.e., the macroscopic deformation was accomplished by the corresponding deformation of the crystalline colloid structure and the particles making up this structure. As reported previously,[29] this means that adhesive and cohesive

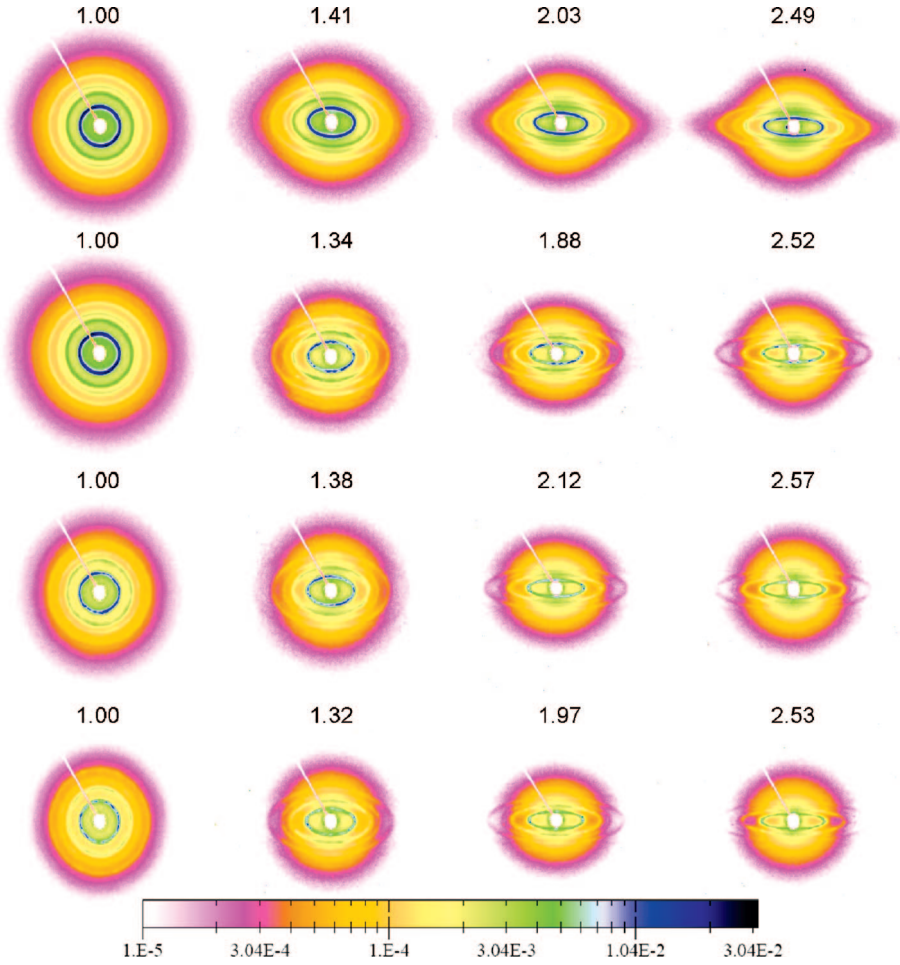

Figure 2. Selected SAXS patterns of uniaxially drawn latex films annealed at 23, 60, 80, and 100 °C (from top to bottom) taken during stretching. The macroscopic draw ratio is indicated on each pattern. The tensile direction is vertical.

forces between latex particles in the film are strong enough to let the whole film behave as a homogeneous system with respect to the externally applied stress field. For samples annealed at room temperature deviation from affine behavior is observed at large draw ratios—in line with earlier observations.[29] Annealing, however, significantly extended the range of draw ratios where affinity of the microscopic deformation with respect to the macroscopic deformation is observed. Affine behavior over the whole range tested is obtained when the sample was annealed at 100 °C. This behavior is explained as follows: It is established that annealing promotes the interdiffusion of the polymeric chains across the boundaries of adjacent latex particles.[37–39] Obviously, the rate of the diffusion of polymeric chains depends on temperature. In the present case the process is slow enough to yield samples in which the interdiffusion proceeded to different (and measurable) extents by simply varying the annealing temperature. Interdiffusion of the polymeric chains enhanced the cohesive bonding between particles in the crystalline lattice as well as at the crystalline grain boundaries. This effectively prevents the slippage of the rows of particles and grain boundaries, resulting in an affine deformation behavior. As a consequence, one also observes an improvement of the mechanical properties as shown in Figure 1. Interestingly, the scattering patterns persist even after annealing at 100 °C, i.e., 80 K above the glass transition temperature. This indicates that the crystalline structure is not dissolved by interdiffusion of the polymeric chains between the constituent latex particles, where the crystalline structure must be defined by the distribution of the non-polymeric material like, e.g., salt and surfactants, between the particles initially composing the film. The results are again in line with the early observations made by Distler and Kanig.[35]

A schematic representation of the deformation mechanism of the latex film while being stretched after being annealed at 23 and 100 °C is presented in Figure 5. The left part of Figure 5 sketches the evolution of the crystalline structure of the closely packed polymer particles at 23 °C. This picture is in line with our previous findings for the nonaffine deformation mechanism.[29] Slippage of rows of particles as well as crystalline grain boundaries passing each other occurs at high deformation ratio due to the limited adhesive and cohesive forces between particles. In this process, capillary forces effectively prevent the formation of voids, keeping the film transparent throughout the experiment. The right part of Figure 5 sketches the structural evolution of the latex film being annealed at 100 °C. One observes completely affine behavior because of the cohesive bonding between particles within crystallites and across crystalline grain boundaries due to the advanced interdiffusion of the polymeric chains caused by annealing.

Conclusion

The effect of annealing on the deformation mechanism in well-ordered styrene/*n*-butyl acrylate copolymer latex films subjected to uniaxial tensile deformation was elucidated. The interpretation of the data relies on the crystalline packing of the polymeric particles which was detected and followed upon stretching by means of synchrotron SAXS measurements. The persistence of the SAXS signal for films even after annealing is attributed to the accumulation of polar polymers on the surface

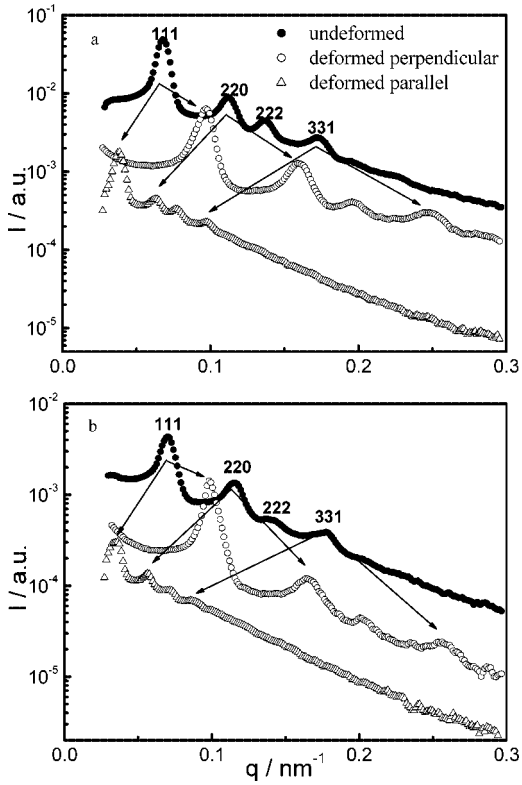

Figure 3. Integrated 1D SAXS intensity distributions of the undeformed latex film and the film after deformation to $\lambda_{m,v} = 2.03$ (top: annealed at 23 °C) and to $\lambda_{m,v} = 1.97$ (bottom: annealed at 100 °C) along directions perpendicular and parallel to the stretching direction. The Miller indices of a fcc crystalline structure are indicated. Arrows indicate the shifts of the (111), (220), and (331) peak positions after deformation.

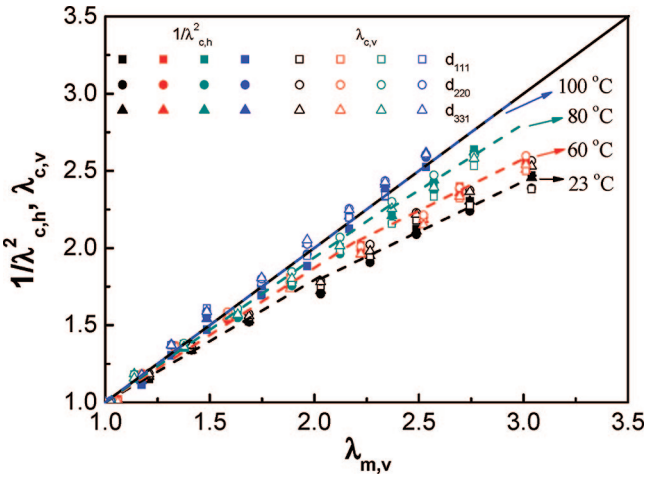

Figure 4. Crystallographic draw and compression ratios of the colloid crystallites along ($\lambda_{c,v}$) and perpendicular ($1/\lambda^2_{c,h}$) to the stretching direction as a function of the macroscopic draw ration ($\lambda_{m,v}$). The solid line indicates the behavior expected for affine deformation. The black, red, dark cyan, and blue symbols stand for samples annealed at 23, 60, 80, and 100 °C, respectively. The respective values are calculated from the shifts in the q positions of the Bragg peaks. Dotted lines are guides for the eyes.

of latex particles, resulting in a retardation of the "oil-in-water" to "water-in-oil" inversion at the last stages of film formation. In the original film nonaffine deformation behavior of the crystalline lattices is attributed to the activation of slips along crystal planes or grain boundaries—in agreement with earlier findings. The polycrystalline structure of latex films was preserved even after annealing for 4 h at temperatures 80 K above the glass transition temperature; i.e., the structure is not completely homogenized by interdiffusion. The deformation mechanism within the latex films transformed from nonaffine deformation to affine deformation behavior after annealing at elevated temperatures. This transformation was attributed to the interdiffusion of polymeric chains between adjacent latex particles, resulting in an enhancement of the cohesive bonding between particles not only within crystalline domains but also at grain boundaries.

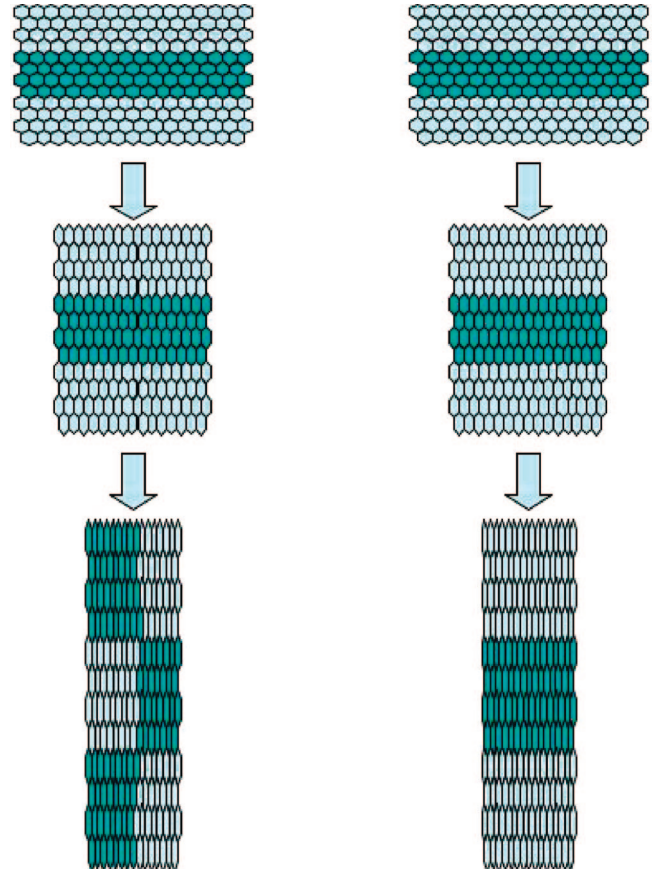

Figure 5. Schematic representation of the structural evolution of the crystalline latex film annealed at 23 (left) and 100 °C (right). Top, undeformed state; middle, at small to moderate deformation; bottom, at large deformation. The marked particles are of a different shade for better visualization of the phenomenon.

Acknowledgment. Y.M. thanks the Hundred Talents Project of the Chinese Academy of Sciences, National Basic Research Program of China (2005CB623800), National Natural Science Foundation of China (50621302), and HASYLAB project II-20052011.

References and Notes

(1) Keddie, J. L. *Mater. Sci. Eng. R* **1997**, *21*, 101.
(2) Steward, P. A.; Hearn, J.; Wilkinson, M. C. *Adv. Colloid Interface Sci.* **2000**, *86*, 195.
(3) Winnik, M. A. *Curr. Opin. Colloid Interface Sci.* **1997**, *2*, 192.
(4) Rieger, J.; Hädicke, E.; Ley, G.; Lindner, P. *Phys. Rev. Lett.* **1992**, *68*, 2782.
(5) Chevalier, Y.; Pichot, C.; Graillat, C.; Joanicot, M.; Wong, K.; Maquet, J.; Lindner, P.; Cabane, B. *Colloid Polym. Sci.* **1992**, *270*, 806.
(6) Roulstone, B. J.; Wilkinson, M. C.; Hearn, J.; Wilson, A. J. *Polym. Int.* **1991**, *24*, 87.
(7) Roulstone, B. J.; Wilkinson, M. C.; Hearn, J. *Polym. Int.* **1992**, *27*, 43.
(8) Wang, Y.; Juhue, D.; Winnik, M. A.; Leung, O. M.; Goh, M. C. *Langmuir* **1992**, *8*, 760.
(9) Xia, Y. N.; Gates, B.; Yin, Y. D.; Lu, Y. *Adv. Mater.* **2000**, *12*, 693.

(10) Bolze, J.; Ballauff, M.; Kijlstra, J.; Rudhardt, D. *Macromol. Mater. Eng.* **2003**, *288*, 495.
(11) Bolze, J.; Ballauff, M.; Rische, T.; Rudhardt, D.; Meixner, A. *Macromol. Chem. Phys.* **2004**, *205*, 165.
(12) Dingenouts, N.; Ballauff, M. *Langmuir* **1999**, *15*, 3283.
(13) Evers, M.; Schope, H.-J.; Palberg, T.; Dingenouts, N.; Ballauff, M. *J. Non-Cryst. Solids* **2002**, *307*, 579.
(14) Petukhov, A. V.; Aarts, D.; Dolbnya, I. P.; de Hoog, E. H. A.; Kassapidou, K.; Vroege, G. J.; Bras, W.; Lekkerkerker, H. N. W. *Phys. Rev. Lett.* **2002**, *88*, 208301.
(15) Hahn, K.; Ley, G.; Schuller, H.; Oberthur, R. *Colloid Polym. Sci.* **1986**, *264*, 1092.
(16) Boczar, E. M.; Dionne, B. C.; Fu, Z. W.; Kirk, A. B.; Lesko, P. M.; Koller, A. D. *Macromolecules* **1993**, *26*, 5772.
(17) Oh, J. K.; Yang, J.; Tomba, J. P.; Rademacher, J.; Farwaha, R.; Winnik, M. A. *Macromolecules* **2003**, *36*, 8836.
(18) Wang, Y. C.; Winnik, M. A. *Macromolecules* **1993**, *26*, 3147.
(19) Liu, Y. Q.; Haley, J. C.; Deng, K.; Lau, W.; Winnik, M. A. *Macromolecules* **2007**, *40*, 6422.
(20) Juhue, D.; Wang, Y. C.; Winnik, M. A.; Haley, F. *Makromol. Chem., Rapid Commun.* **1993**, *14*, 345.
(21) Kawaguchi, S.; Odrobina, E.; Winnik, M. A. *Macromol. Rapid Commun.* **1995**, *16*, 861.
(22) Ye, X. D.; Wu, J.; Oh, J. K.; Winnik, M. A.; Wu, C. *Macromolecules* **2003**, *36*, 8886.
(23) Kim, H. B.; Winnik, M. A. *Macromolecules* **1994**, *27*, 1007.
(24) Kim, H. B.; Winnik, M. A. *Macromolecules* **1995**, *28*, 2033.
(25) Juhue, D.; Lang, J. *Macromolecules* **1995**, *28*, 1306.
(26) Lepizzera, S.; Pith, T.; Fond, C.; Lambla, M. *Macromolecules* **1997**, *30*, 7945.
(27) Lepizzera, S.; Scheer, M.; Fond, C.; Pith, T.; Lambla, M.; Lang, J. *Macromolecules* **1997**, *30*, 7953.
(28) Rharbi, Y.; Boue, F.; Joanicot, M.; Cabane, B. *Macromolecules* **1996**, *29*, 4346.
(29) Men, Y. F.; Rieger, J.; Roth, S. V.; Gehrke, R.; Kong, X. M. *Langmuir* **2006**, *22*, 8285.
(30) Oberdisse, J. *Macromolecules* **2002**, *35*, 9441.
(31) Oberdisse, J.; Deme, B. *Macromolecules* **2002**, *35*, 4397.
(32) Hu, S. S.; Men, Y. F.; Roth, S. V.; Gehrke, R.; Rieger, J. *Langmuir* **2008**, *24*, 1617.
(33) Bradford, E. B.; Vanderhoff, J. W. *J. Macromol. Chem.* **1966**, *1*, 335.
(34) Bradford, E. B.; Vanderhoff, J. W. *J. Macromol. Sci., Phys.* **1972**, *B6*, 671.
(35) Distler, D.; Kanig, G. *Colloid Polym. Sci.* **1978**, *256*, 1052.
(36) Rieger, J.; Dippel, O.; Hädicke, E.; Ley, G.; Lindner, P. In *Colloidal Polymer Particles*; Buscall, R., Goodwin, J. W., Eds.; Academic Press: London, 1994; p 29.
(37) Ye, X. D.; Farinha, J. P. S.; Oh, J. K.; Winnik, M. A.; Wu, C. *Macromolecules* **2003**, *36*, 8749.
(38) Perez, E.; Lang, J. *Langmuir* **2000**, *16*, 1874.
(39) Wang, Y. C.; Zhao, C. L.; Winnik, M. A. *J. Chem. Phys.* **1991**, *95*, 2143.

MA800435F